The LHCb SMOG system

Chiara Lucarelli

on behalf of the LHCb collaboration

LHC Forward Physics 2024,
15 July 2024, CERN

The LHCb experiment

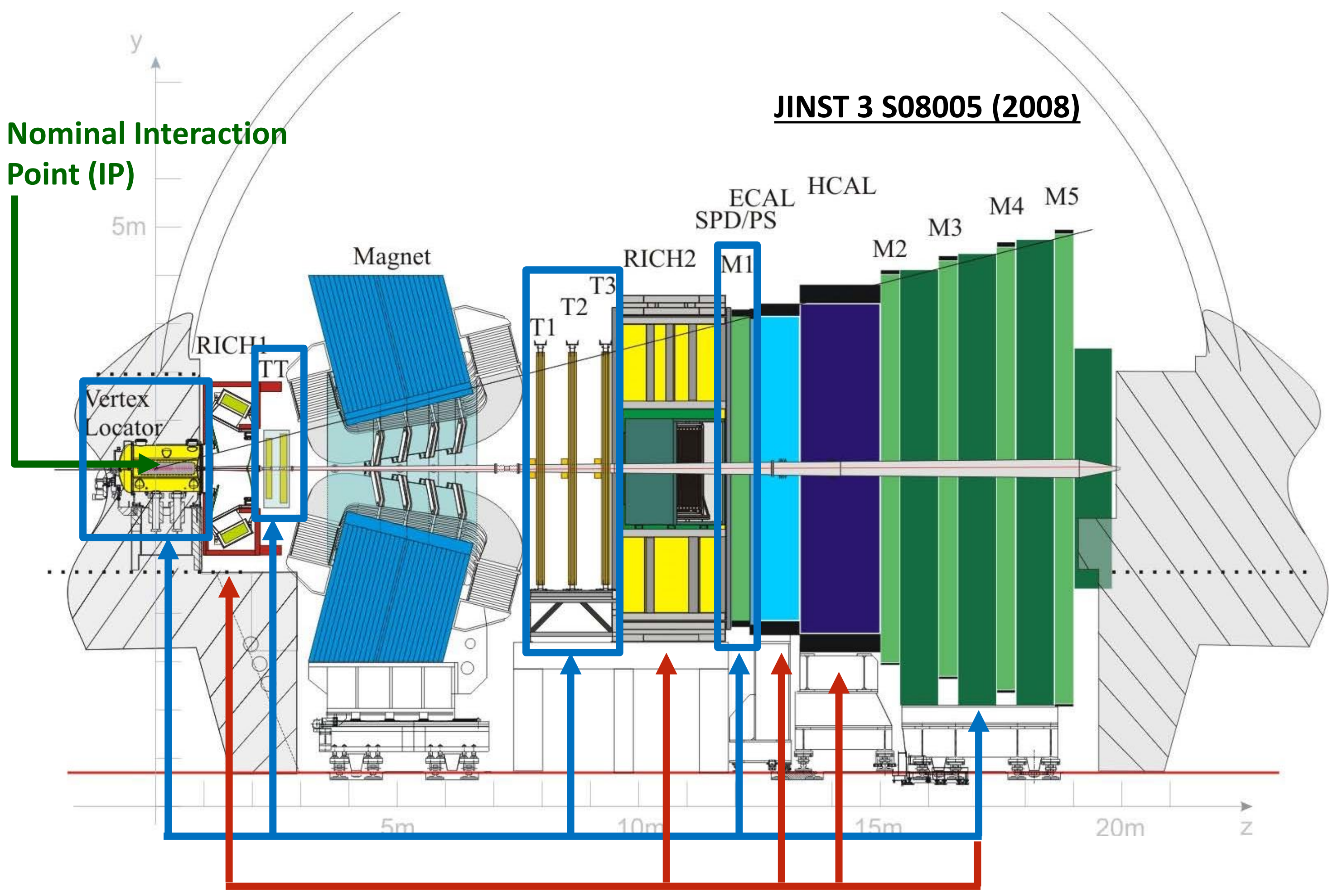

The LHCb is a general-purpose experiment in the forward direction:

- **Single-arm forward spectrometer**: optimized for $b\bar{b}$ production, $2 < \eta < 5$, $\Theta \in [10, 250]$ mrad.
- **Tracking:** excellent vertexing, IP resolution: 15+29/p_T [GeV] µm, momentum resolution: $\Delta p/p = 0.5\% - 1.0\%$.
- **Particle Identification (PID):** excellent separation among K, π and p with momentum in [10, 110] GeV/c range.
- **Trigger:** flexible and versatile, bandwidth up to 15 kHz to disk.
- Its forward geometry is very well suited for **fixed-target physics.**

LHCb fixed-target apparatus

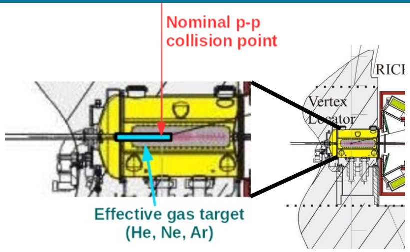

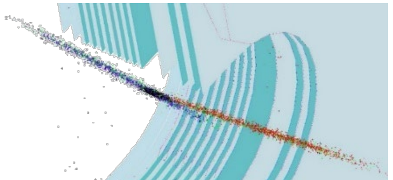

JINST 9 (2014) P12005

SMOG: The *System for Measuring Overlap with Gas*

- Inject noble gases (He, Ne, Ar) in LHC beam pipe around (±20 m) the LHCb IP, pressure of **2x10^{-7} mbar** (x100 nominal LHC vacuum)
- Since 2015, exploited for LHCb fixed-target physics programme: **highest-energy fixed-target experiment ever.**

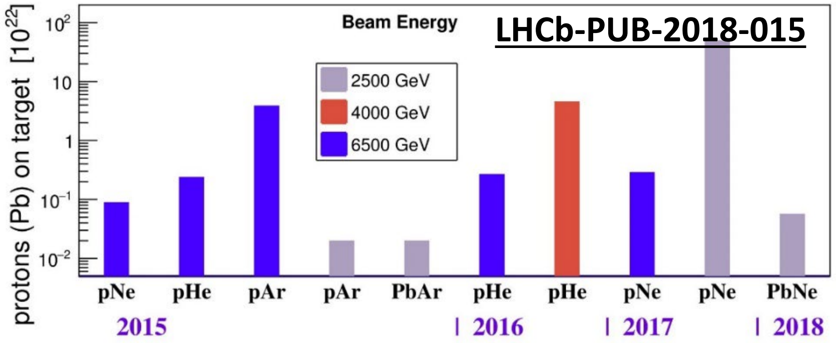

Unique physics opportunities at the LHC

- Unexplored **intermediate energy** to SPS and LHC: $\sqrt{s_{NN}} \in [30, 115]$ GeV
- **Large target Bjorken-*x* at intermediate Q^2**
- Collisions with **targets of mass number A intermediate** between *p* and Pb

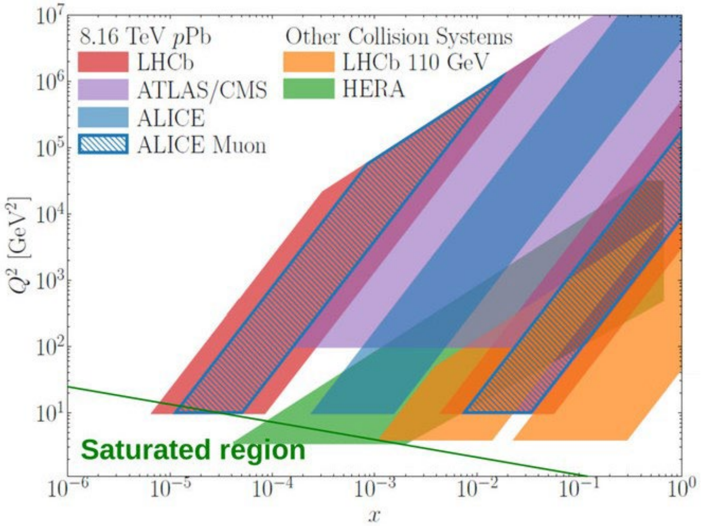

- **Cold nuclear-matter effects (CNM)** for QGP studies
- **Nuclear PDFs at high-*x*** and strange hadronization process
- **Hadron production** and spectra measurements for CRs physics
- **Polarization studies** in baryon production

Antimatter production for Cosmic Rays physics

Detached antiproton production

Eur. Phys. J. C83 (2023) 543

- **Interpretation of $\bar{p}$ flux in CRs** measurement (indirect DM searches) **limited by models of $\bar{p}$ production** in CRs collisions with the interstellar medium (H, He)
- **Dedicated measurement to the component from anti-hyperon decays** (20-30% of $\bar{p}$ production) in *p*He, extending first LHCb result only dealing with the prompt processes [PRL 121 (2018) 222001] → Two complementary approaches

Exclusive

$$R_{\bar{\Lambda}} = \frac{\sigma(\mathrm{pHe} \to (\bar{\Lambda}_{\mathrm{prompt}} \to \bar{p}\pi^+)X)}{\sigma(\mathrm{pHe} \to \bar{p}_{\mathrm{prompt}}\, X)}$$

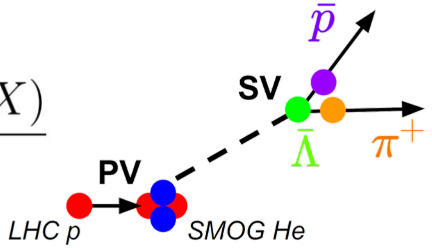

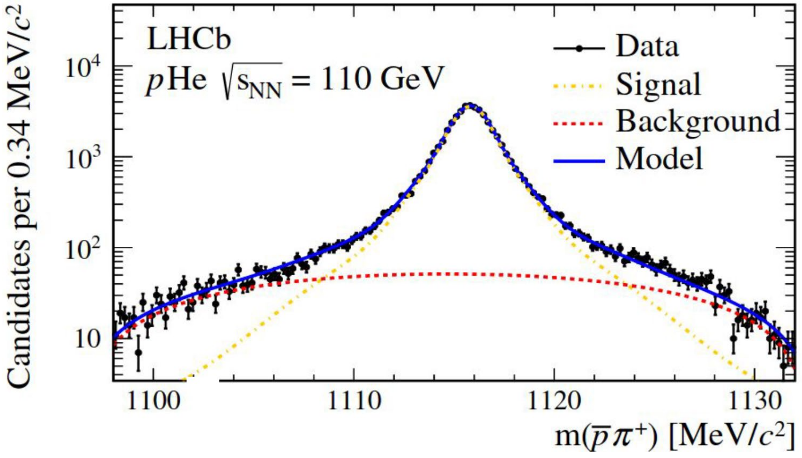

Inclusive

$$R_{\bar{H}} \equiv \frac{\sigma(\mathrm{pHe} \to \bar{H}X \to \bar{p}X)}{\sigma(\mathrm{pHe} \to \bar{p}_{\mathrm{prompt}}X)}, \quad \bar{H} = \bar{\Lambda}, \bar{\Sigma}, \bar{\Xi}, \bar{\Omega}$$

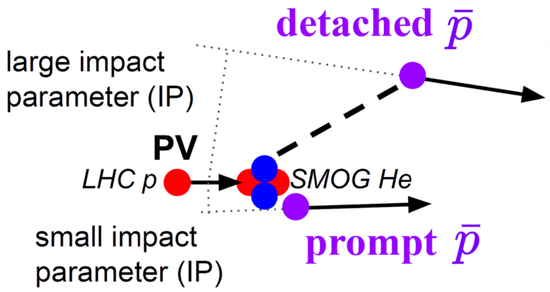

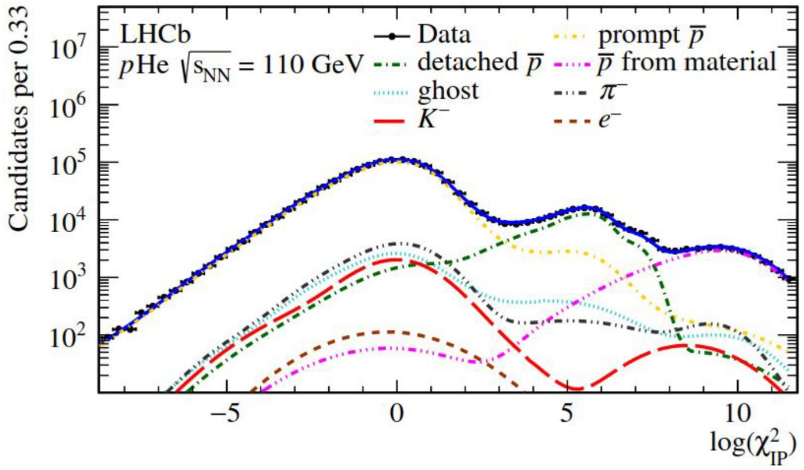

Results

Eur. Phys. J. C83 (2023) 543

Larger contribution measured wrt all most widely used theoretical models

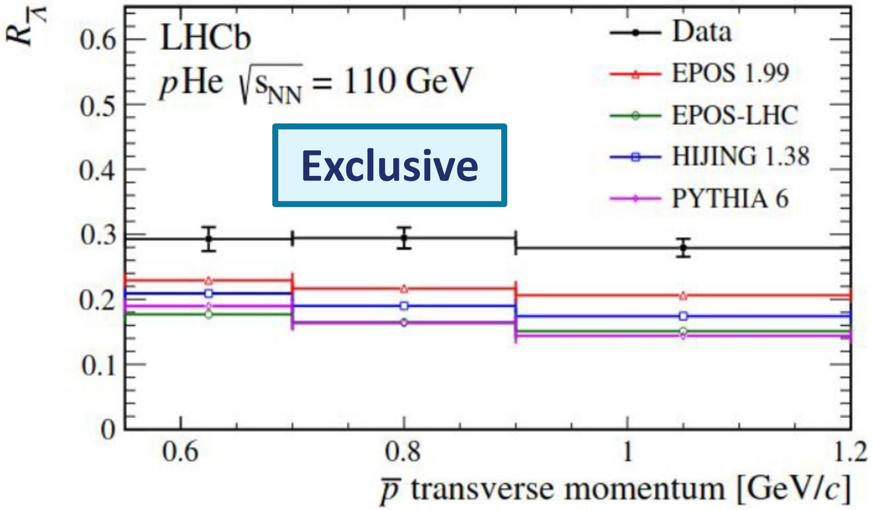

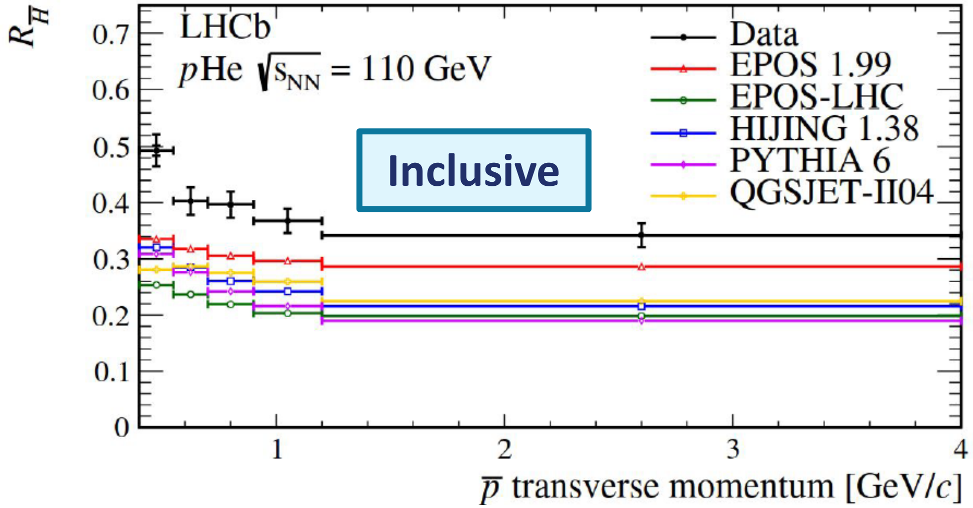

- Ratio of the results is expected to be **predicted more reliably** than the single terms (depends only on the hadronization).
- Results mutually cross-checked since found to be **consistent with EPOS-LHC prediction.**

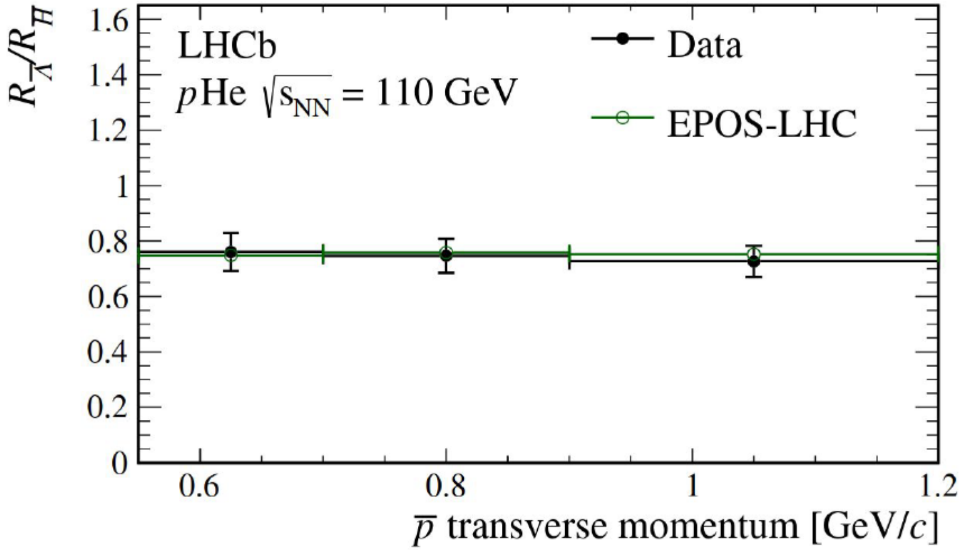

Light (anti-)nuclei identification

Expand antimatter **production** measurements to **light anti-nuclei**:

- No known primary sources
- Low production cross-section in secondary collisions

LHCb not designed to identify light (anti-)nuclei

→ **New techniques under development.**

LHCb-DP-2023-002

1 **Ionisation losses** in silicon sensors: **Z^2 dependence** in Bethe-Bloch → dE/dx to **identify He**

***pp* at $\sqrt{s}$ = 13 TeV**, $\mathcal{L}_{int}$=5.5 fb^{-1}

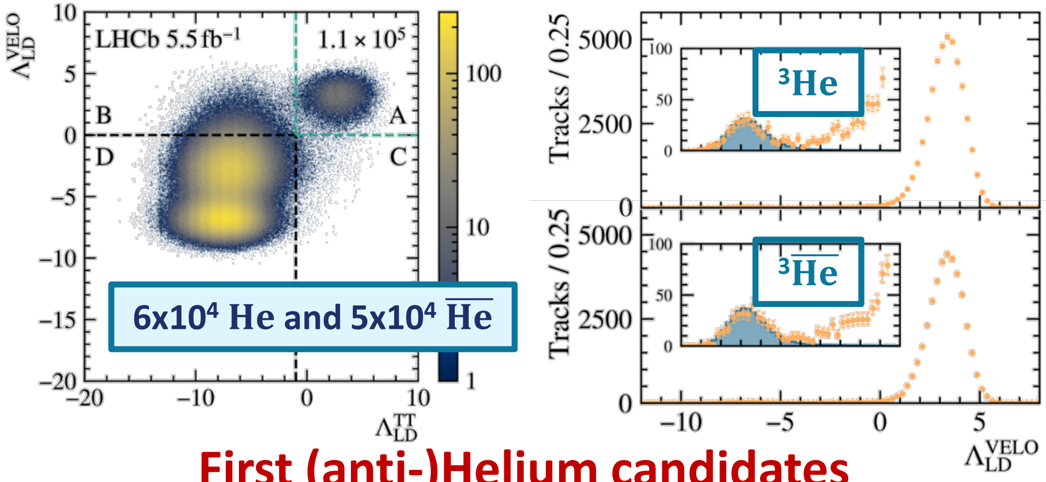

First (anti-)Helium candidates observed in *pp* in LHCb data!

LHCb-FIGURE-2023-017

2 Light nuclei slower than c: **M dependence** of particle speed → **Time-of-flight** to **identify d, distinguish ^{3}He and ^{4}He**

~10% of SMOG *p*He ($\sqrt{s_{NN}}$ = 110 GeV)

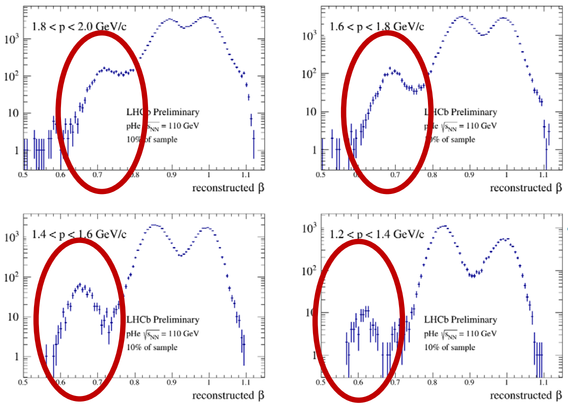

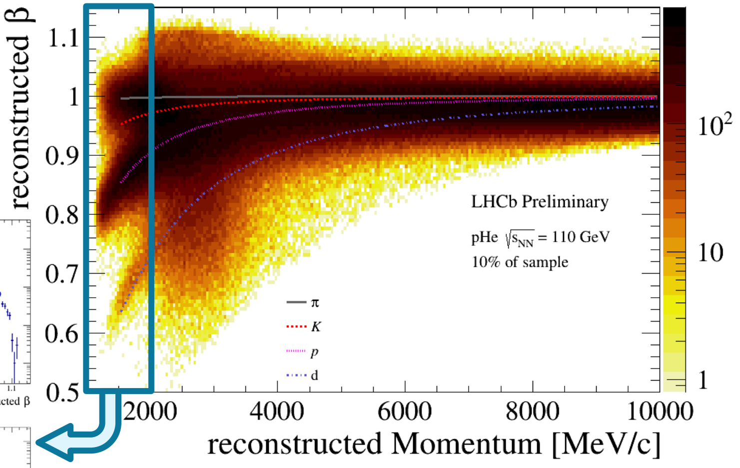

First deuteron candidates observed in *p*He data!

Charm production in *p*Ne and PbNe

Charm production in fixed-target

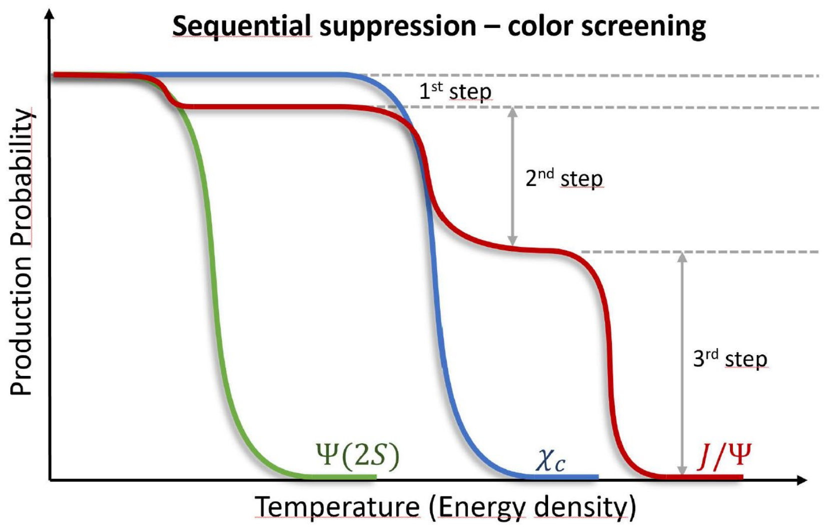

Quarkonia dissociation due to colour charge screening is a predicted signature of QGP formation: measurement of **sequential suppression** mechanism corrected for CNM **smoking gun for QGP**

→ Measurements of **charmonia production** in different nuclear systems and kinematic phase space crucial **to quantify Cold Nuclear Matter effects**

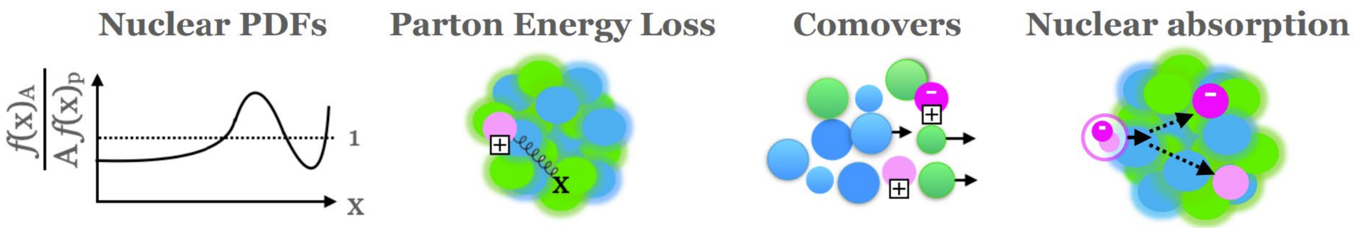

Measurement of D^0, J/ψ and ψ(2s) in *p*Ne and D^0 and J/ψ in PbNe $\sqrt{s_{NN}}$=68 GeV

- Unique energy scale
- Sensitive to possible nucleon intrinsic charm (IC) content
- Extend previous D^0 and J/ψ measurements in *p*He (110 Gev) and *p*Ar (68 GeV) [PRL 122 (2019) 132002]

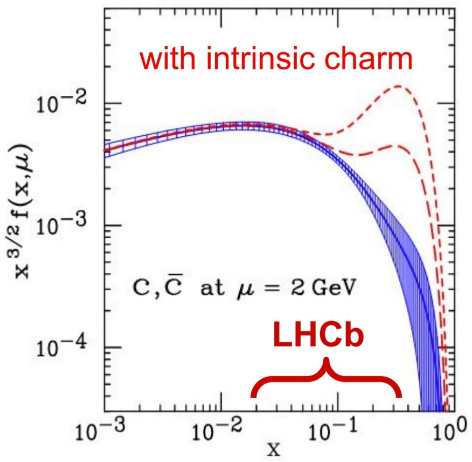

Phys Rec D75 054029

Results

pNe Eur. Phys. J. C83 (2023) 625

- **Good agreement with Vogt** predictions (**no IC, 1% IC**)
- **J/ψ** cross-section **in agreement with previous experiments**
  → **Power law dependence** on centre of mass energy
- ψ(2S)/ J/ψ ratio compatible with previous measurements with similar A.

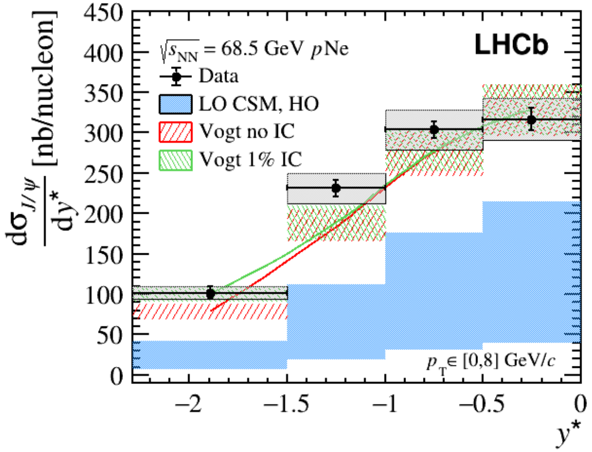

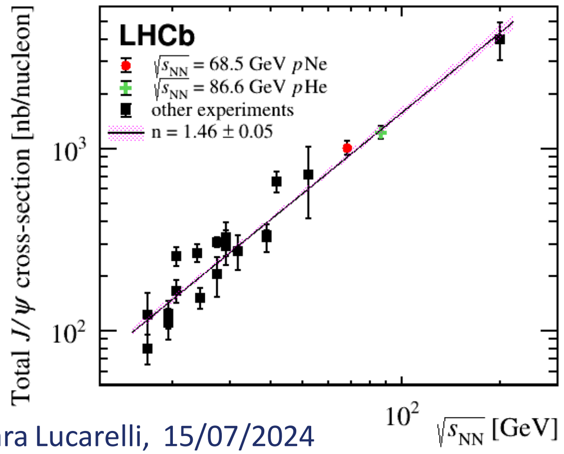

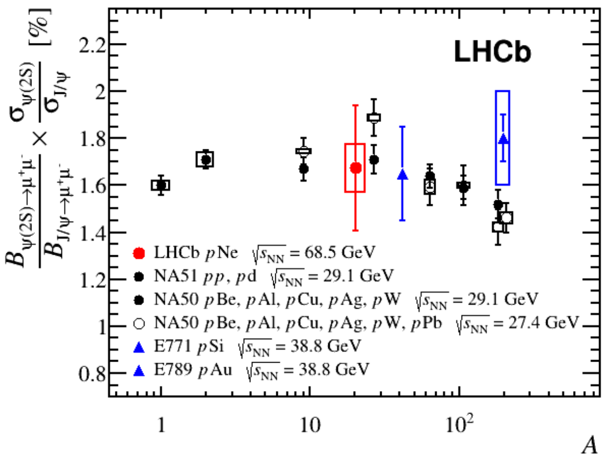

PbNe Eur. Phys. J. C83 (2023) 658

- Unique opportunity to **measure J/ψ to D^0 ratio at LHC correcting for CNM**.
- Ratio as function of collisions N_{coll} is power law

$$\frac{\sigma_{J/\psi}}{\sigma_{D^0}} = \frac{\sigma^{pp}_{J/\psi}}{\sigma^{pp}_{D^0}} \times \langle N_{coll} \rangle^{\alpha'-1}$$

- N_{coll} from Glauber model to ECAL energy deposits.
  → **α'<1**: additional nuclear effects on J/ψ
  → Same trend between *p*Ne and central PbNe: **no evidence for anomalous suppression.**

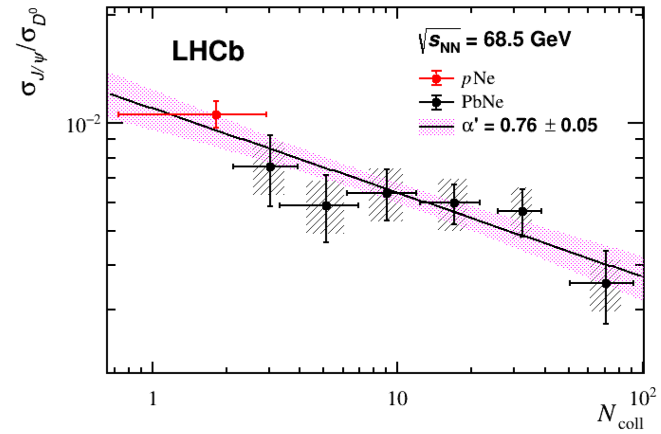

Λ^0 transverse polarization

Λ^0 transverse polarization

First observation of Λ^0 transverse polarization (1976):
non perturbative spin effects even in high energy collisions.

Experimental measurements highlighted common features:

- Polarization **increases with x_F and p_T** up to few GeV
- **Independent of beam energy** and colliding system
- **Same magnitude** of polarization observed **for other hyperons**

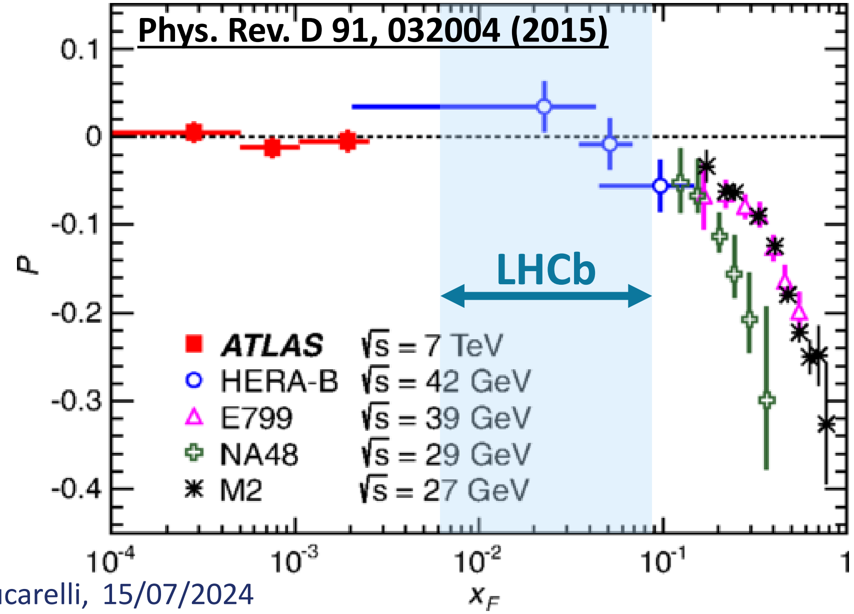

Study polarization in *p*Ne $\sqrt{s_{NN}}$=68 GeV

Same x_F coverage as HERA-B but higher energy
→ Study energy (in)dependence of polarization

Exploit self-analysing decays $\boldsymbol{\Lambda^0 \longrightarrow p\pi^-}$ and $\boldsymbol{\overline{\Lambda}^0 \longrightarrow \overline{p}\pi^+}$:

- **Strong parity violation:** *p* preferentially emitted along the Λ^0 spin direction in its rest frame.

  → Protons angular distribution depends on the Λ^0 polarization P^{Λ^0}

P^{Λ^0} from linear fit of *p* angular distribution in bin of cosθ

Polarization studied as a function of the Λ^0 p_T , η, *y* and x_F considering dependence observed in previous studies.

$$\frac{dN}{d\Omega} = \frac{dN_0}{d\Omega}(1 + \alpha P^{\Lambda^0} \cos\theta)$$

Results

arXiv:2405.11324, submitted to JHEP

Kinematic range: 300< p_T <3000 MeV/c & 2<η<5

$P(\Lambda^0) = 0.029 \pm 0.019 \pm 0.012$

$P(\overline{\Lambda}^0) = 0.003 \pm 0.023 \pm 0.014$

Uncertainty dominated by limited statistic.

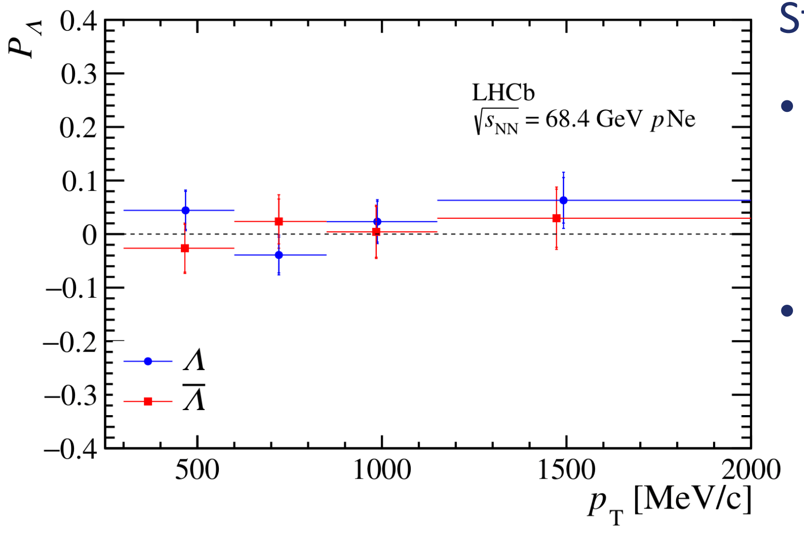

Study performed in kinematic bin:

- Λ^0: **increasing trend** in polarity, compatible with previous experiments.
- $\overline{\Lambda}^0$: **flat distribution around 0**

→ Compatible with previous experiments, in contrast with theoretical expectations.

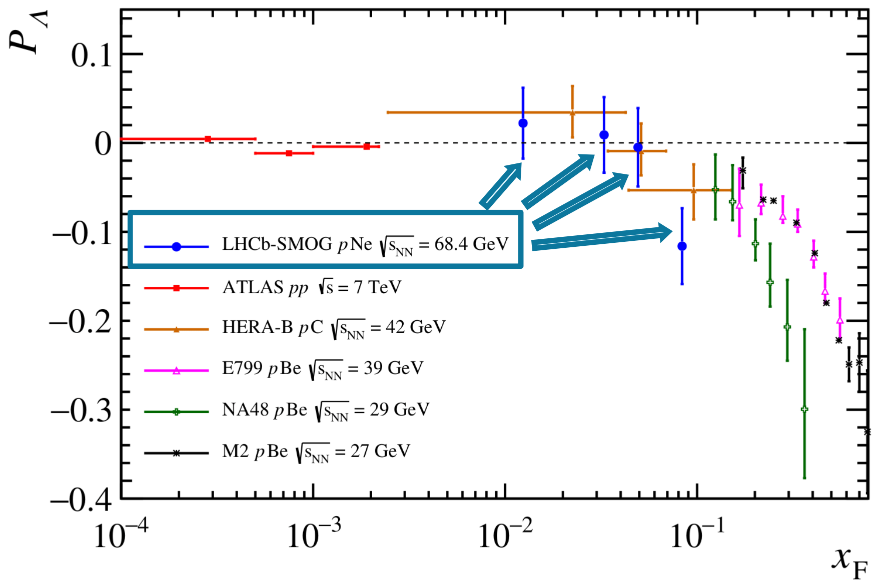

Comparison of results as a function of x_F with previous experiments:

- Different kinematical regions and collision systems
- **Very good agreement in polarization values**.

Fixed-target upgrade for Run 3

SMOG upgrade: SMOG2

SMOG2: gas confined in a 20 cm long storage cell upstream the interaction point:

- **x100 average pressure** with same gas flow
- Direct and precise gas pressure and temperature measurements
- **Simultaneous *pp* + fixed-target data taking**
- Wider choice of injectable gases: **H_2, D_2, N_2, O_2**, Kr, Xe (+He, Ne, Ar)

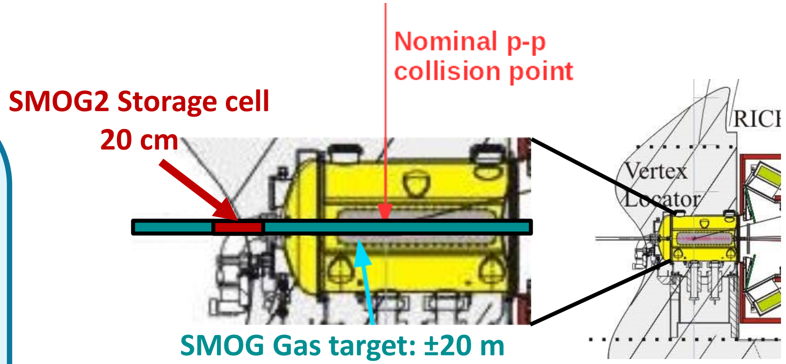

LHCb-FIGURE-2023-001

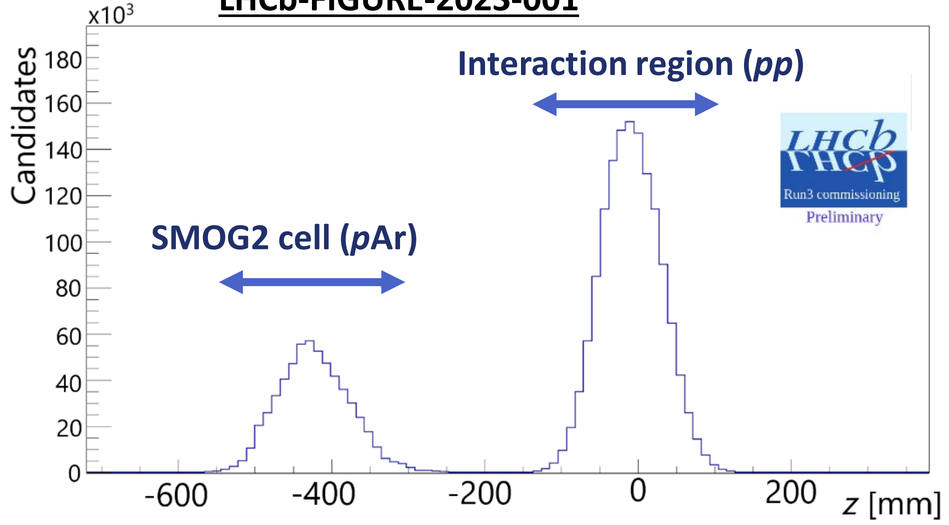

LHCb-FIGURE-2024-005

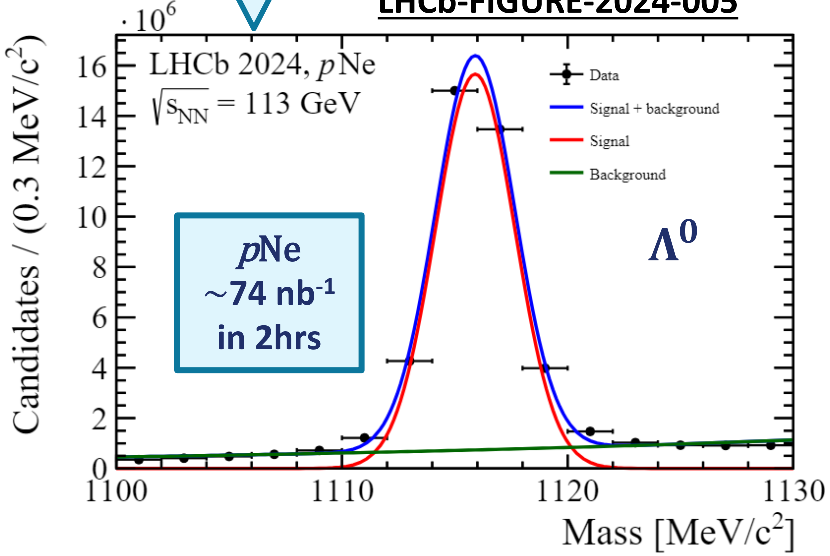

SMOG upgrade: SMOG2

LHCb-FIGURE-2024-005

Data samples collected during April and May 2024 with all available gases!

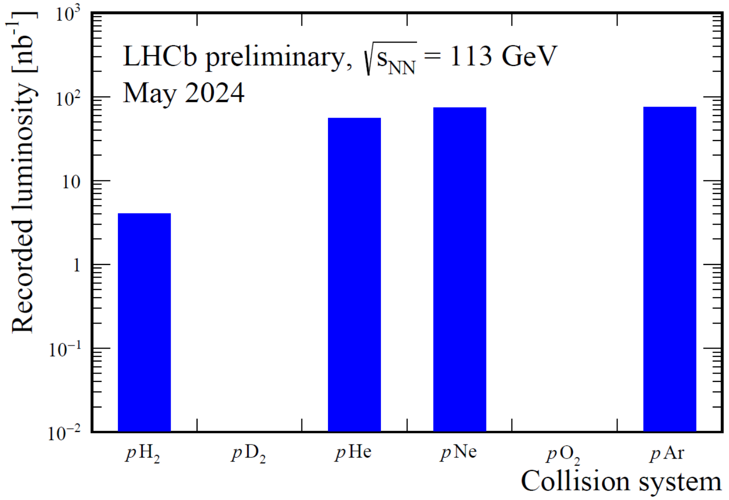

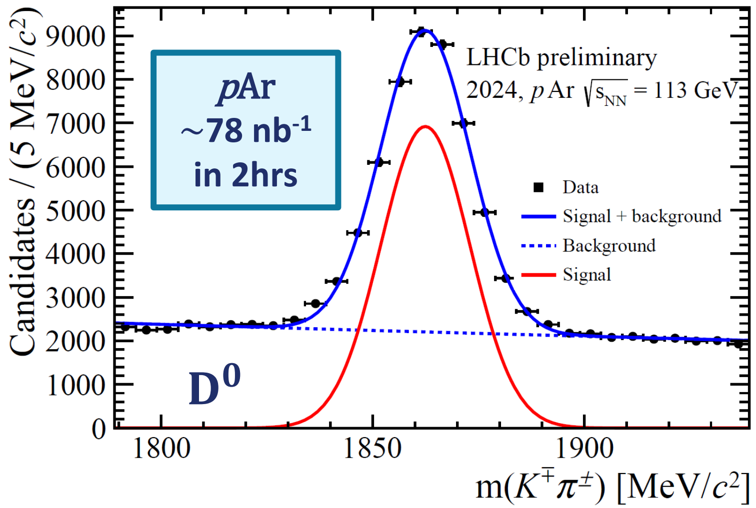

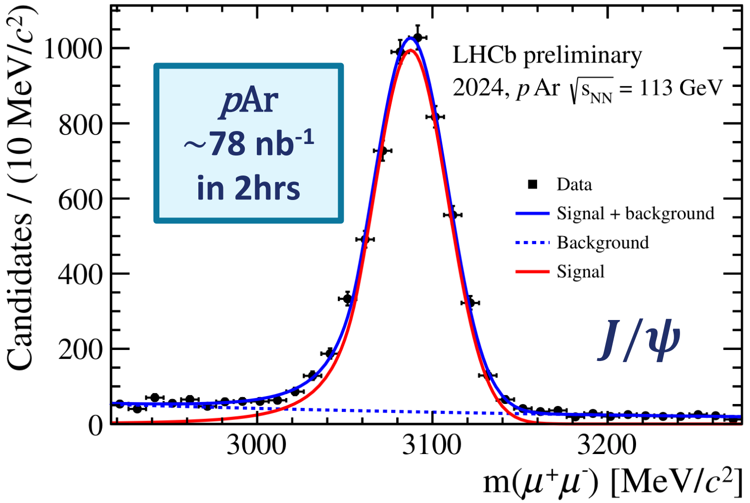

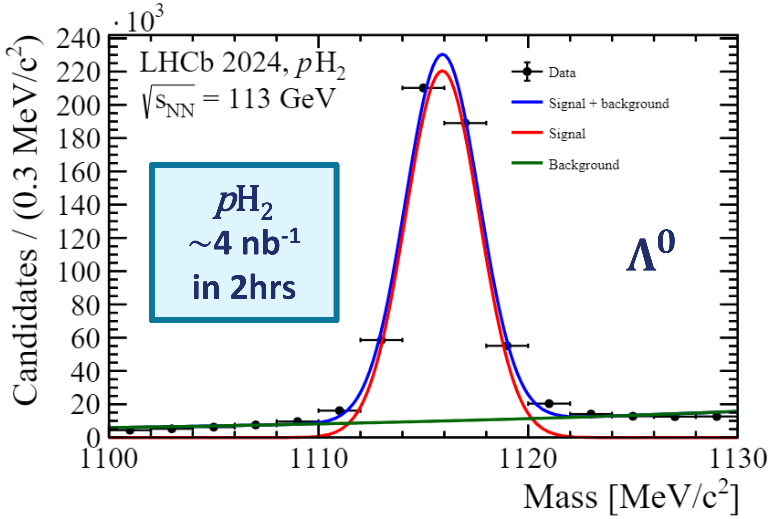

Unique physics opportunities never explored at LHC:

- **Charmonium, bottomonia and exotica production** from H_2 to Kr.
- pH_2, pHe, pD_2, pO_2 and OH_2 collisions to extend **modelling of productions of CR interest.**
- **Flow measurements** at low energy over wide pseudorapidity range.
- **Ultra-peripheral collisions** in pA and PbA.

Conclusions

LHCb can perform the highest-energy fixed-target measurement ever

- **Measurement of detached-to-prompt $\bar{p}$ production in *p*He collisions**
  - Together with prompt $\bar{p}$ production measurement, anti-hyperon contribution to $\bar{p}$ production crucial input to models of antimatter production in space
- **Open and hidden charm measurements in *p*Ne and PbNe collisions**
  - Unexplored energy scale, unique possibility to measure charmonia production **correcting for CNM**.
- **First LHCb Λ^0 polarization measurement in *p*Ne collisions**
  - Unexplored kinematic region, contributing to understand the long-standing challenge of the transverse Λ^0 polarization explanation.

Many more interesting results in store with SMOG2 data samples!

Thanks for the attention!

BACKUP

Prompt antiproton production

PRL 121 (2018) 222001

First measurement of $\boldsymbol{\sigma(pHe \longrightarrow \bar{p}_{prompt}X)}$ at $\sqrt{s_{NN}} = 110\ GeV$:

- $\bar{p}$ reconstructed in the kinematic region $p \in [12{,}110]\ GeV/c$, $p_t \in [0.4, 4]\ GeV/c$ to optimize reconstruction and particle identification efficiencies.
- **Only $\bar{p}$ promptly produced** considered; detached component reduced cutting on the impact parameter wrt the primary vertex.
- $\bar{p}$ number from a simultaneous fit to the PID variables in (p, p_t) bins.
- Luminosity from $\boldsymbol{pe}$ **elastic scattering** with gas atomic electrons.

→ **Dominant contribution to systematic:**

- **Luminosity measurement: injected gas pressure not precisely measured.**
- **Particle identification performance: poor calibration statistics.**

- Result on XS is compared to different MC event generator.
- **Experimental uncertainties (<10%) are lower than the spread among theoretical models**.

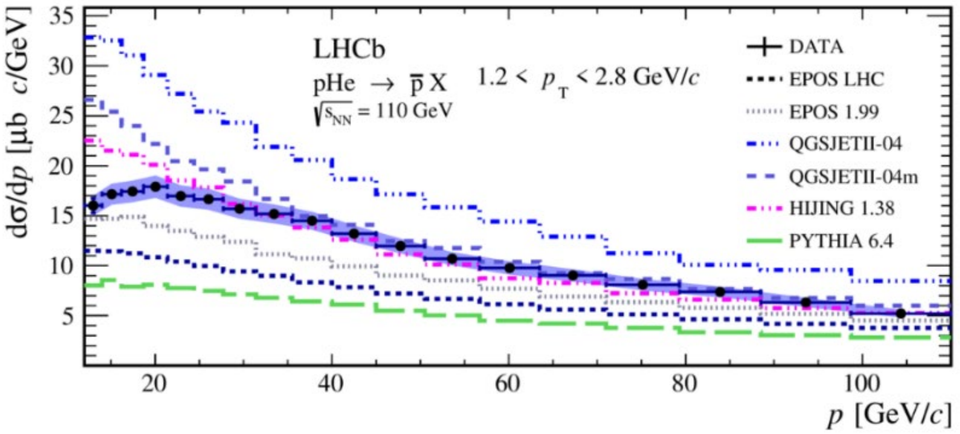

Impact of the measurement

Important contribution to the improvement of the secondary $\overline{p}$ flux prediction:

- Validation of the extrapolation of the cross section from pp to pHe.
- Validate models for the cross section energy evolution (violation of Feynman scaling above 50 GeV).

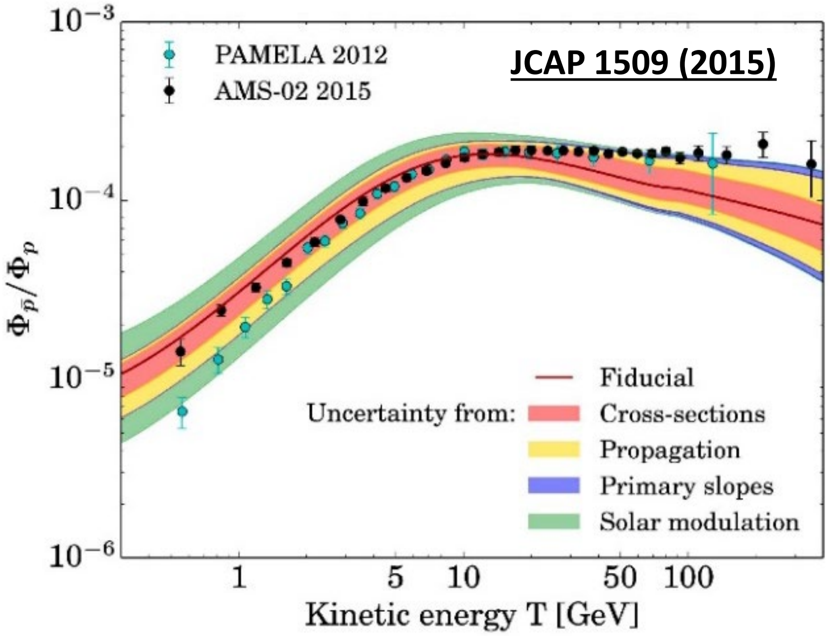

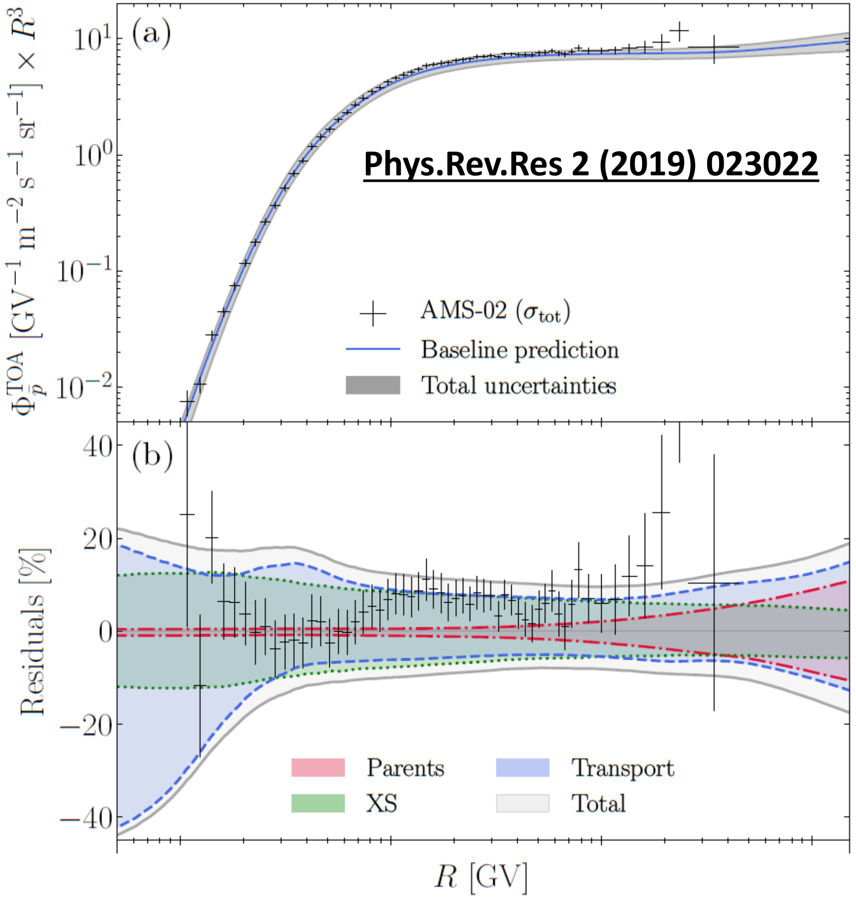

- **The uncertainty on the predicted secondary $\overline{p}$ flux is reduced.**
- **Room for exotic contribution heavily reduced**

Luminosity measurement in SMOG data samples

PRL 121 (2018) 222001

SMOG is not equipped with precise gauges for the gas pressure:

→ Luminosity is determined through ***pe* elastic scattering** with gas atomic electrons.

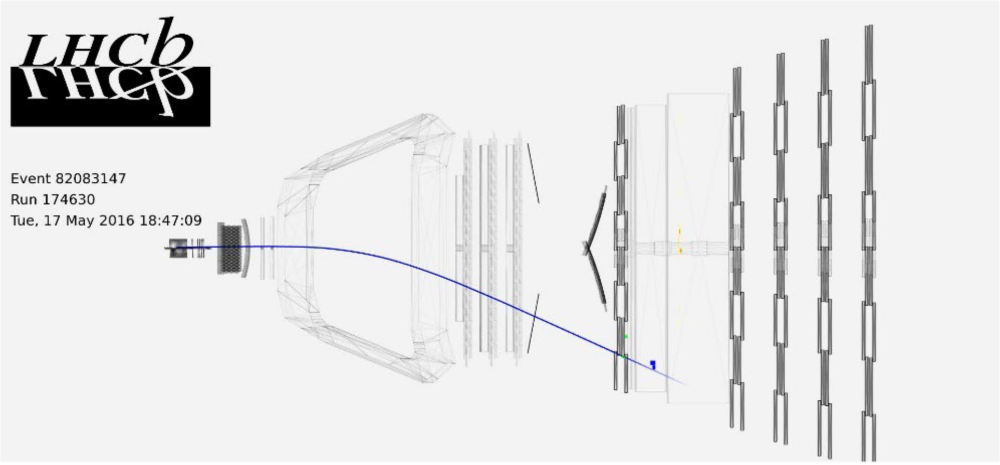

- pe events are identified as an isolated low-energy electron track.
- Charge symmetric background is evaluated through positron yield and subtracted from electron yield.
- Poor electron reconstruction efficiency (16%) → 6% uncertainty on luminosity

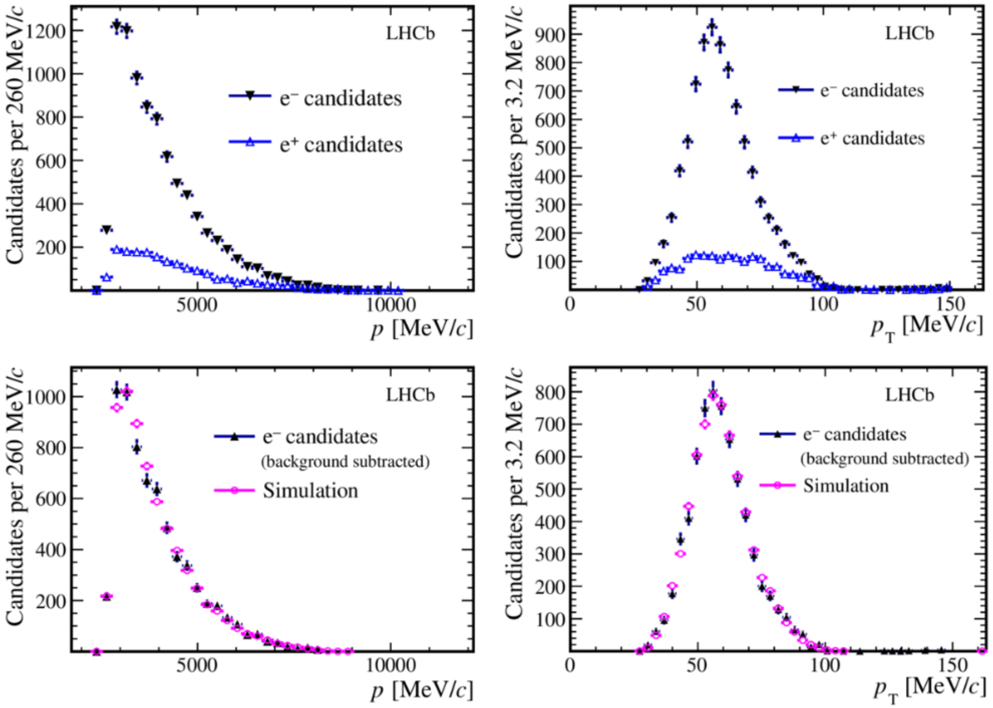

Dominant contribution to systematic uncertainty on σ!

Detached antiproton production

- Interpretation of $\bar{p}$ flux in CRs measurement (indirect DM searches) limited by models of $\bar{p}$ production in CRs collisions with the interstellar medium (H, He)
- Dedicated measurement to the component from anti-hyperon decays in pHe, extending first LHCb result only dealing with the prompt processes → Around **20-30% of $\bar{p}$ production** comes from anti-hyperon decays:

$$\bar{\Lambda}^0_{\text{prompt}} \to \bar{p}\pi^+ \qquad \bar{\Sigma}^- \to \bar{p}\pi^0 \qquad \bar{\Xi}^+ \to \bar{\Lambda}\pi^+ \qquad \bar{\Xi}^0 \to \bar{\Lambda}\pi^0 \qquad \bar{\Omega}^+ \to \bar{\Lambda}K^+$$

- Available data indicate strangeness enhancement but **large spread among different theoretical models**

→ **LHCb SMOG measurement can constrain the models**

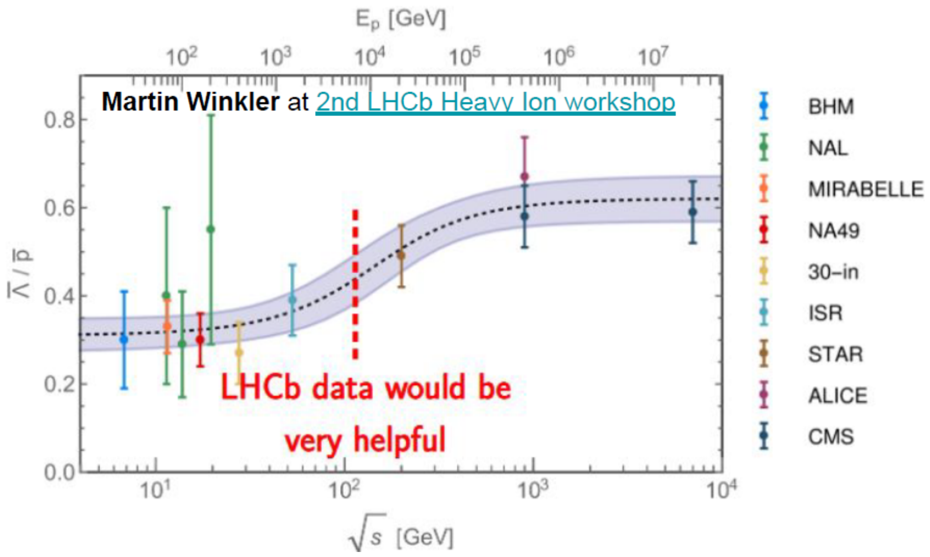

CERN-THESIS-2021-313

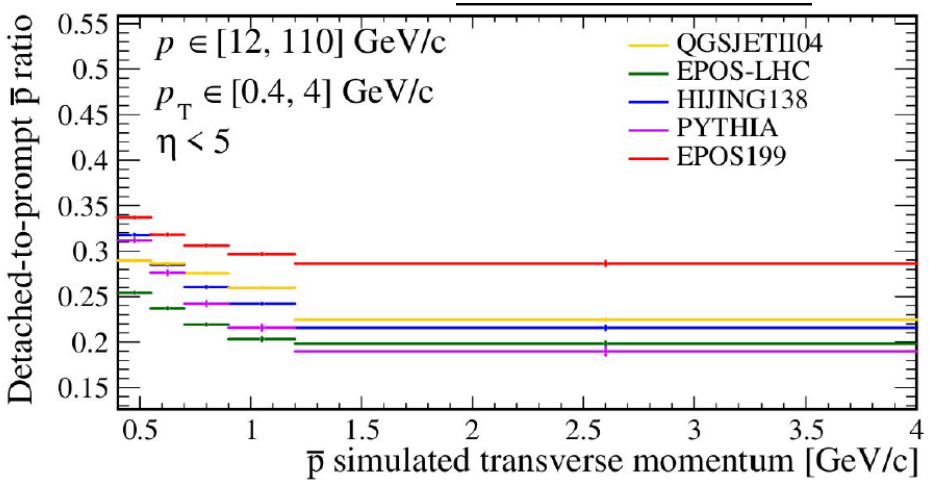

Analysis strategy

[Eur. Phys. J. C83 (2023) 543]

Analysis for secondary-to-primary $\bar{p}$ ratio $\boldsymbol{R = \sigma_{sec}/\sigma_{prim}}$ following **two complementary approaches**:

- **Exclusive approach**: $R_{\bar{\Lambda}} = \dfrac{\sigma(p\mathrm{He} \to (\bar{\Lambda}_{\mathrm{prompt}} \to \bar{p}\pi^{+})X)}{\sigma(p\mathrm{He} \to \bar{p}_{\mathrm{prompt}}\, X)}$
  - Measure $\boldsymbol{\bar{\Lambda} \longrightarrow \bar{p}\pi^{+}}$, dominant detached component.
  - Identifying decay exploiting LHCb **excellent mass resolution** (no PID info): event selection via **kinematic description in the Armenteros plot** and **impact parameters**.
  - Most systematic uncertainties (luminosity, reco, …) **cancel in the ratio**.

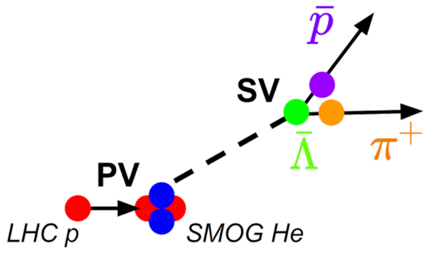

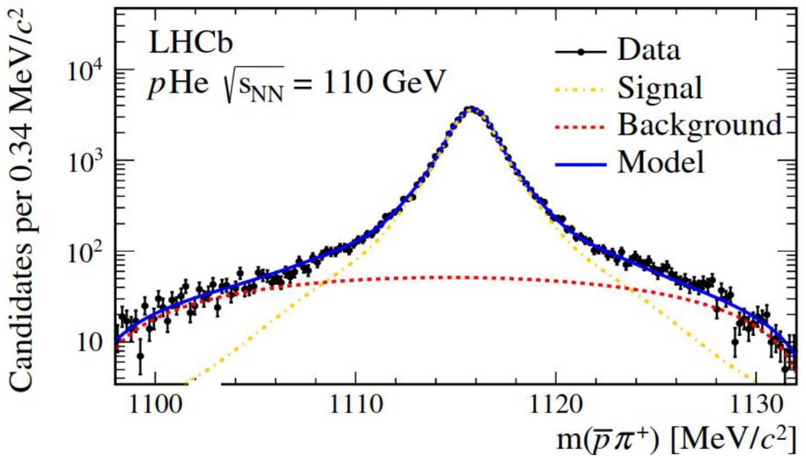

- **Inclusive approach**: $R_{\bar{H}} \equiv \dfrac{\sigma(p\mathrm{He} \to \bar{H}X \to \bar{p}X)}{\sigma(p\mathrm{He} \to \bar{p}_{\mathrm{prompt}} X)}$, $\bar{H} = \bar{\Lambda}, \bar{\Sigma}, \bar{\Xi}, \bar{\Omega}$
  - Focused on **all detached components.**
  - Selecting $\boldsymbol{\bar{p}}$ **with tight PID cuts**
  - Distinguishing between prompt, detached and secondary $\bar{p}$ via a **fit to the *p*He data impact parameter** with the composition of templates.

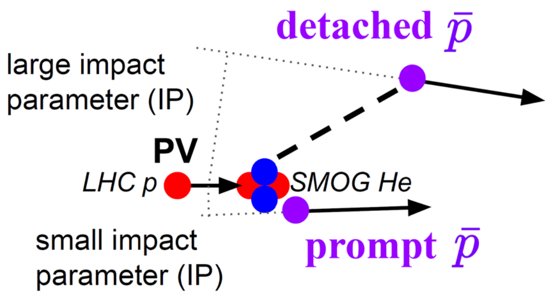

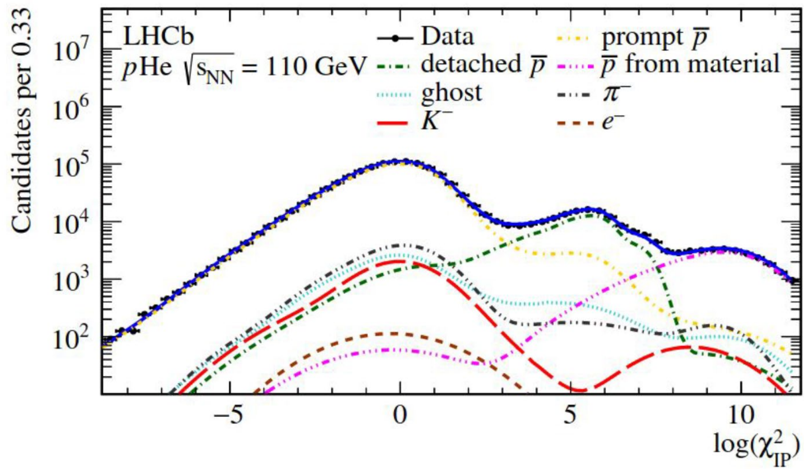

Results

Eur. Phys. J. C83 (2023) 543

Larger contribution measured wrt all most widely used theoretical models

Exclusive

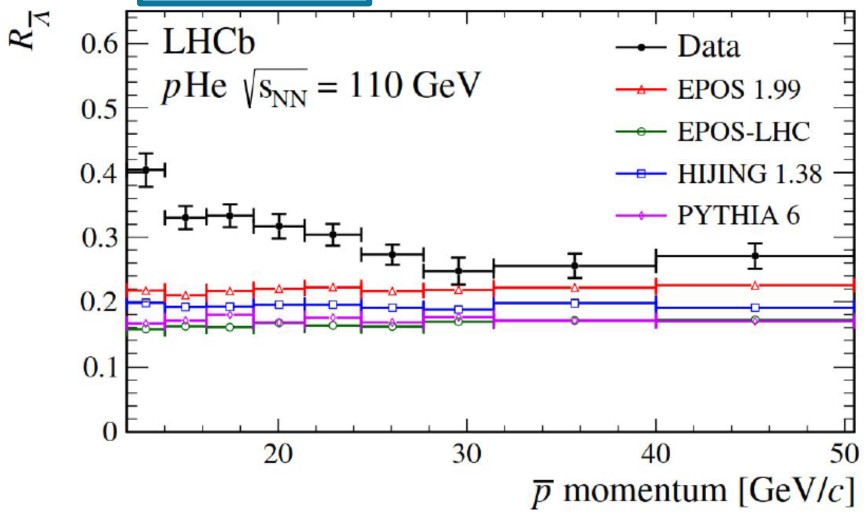

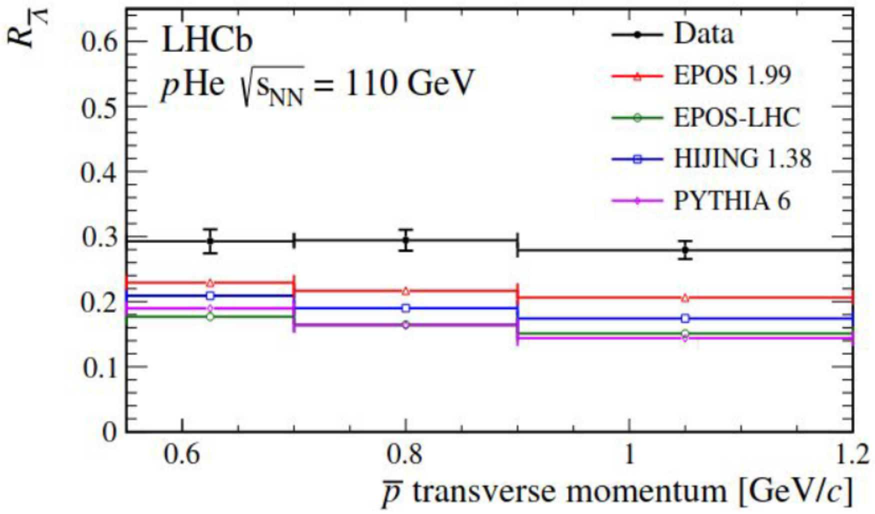

EPOS 1.99: Nuclear Physics B.2009.09.017
EPOS-LHC: Phys. Rev. C 92,034906
HIJING 1.38: Computer Physics Communications 83 (1994) 307-331
PYTHIA 6: JHEP 05 (2006) 026

Inclusive

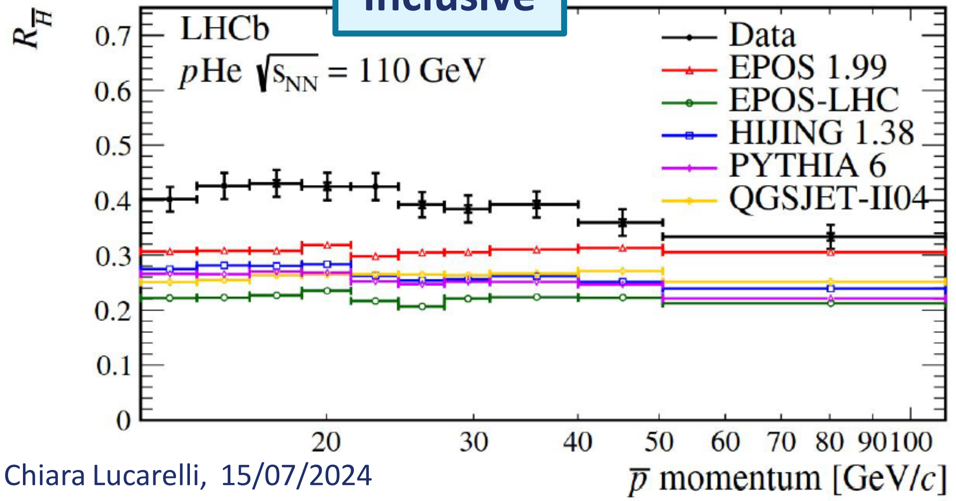

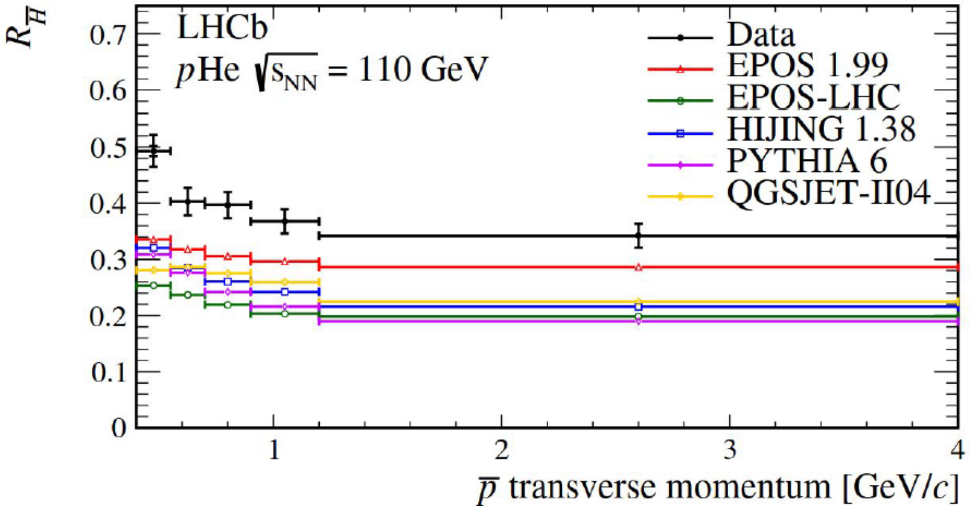

(Anti-)Helium identification

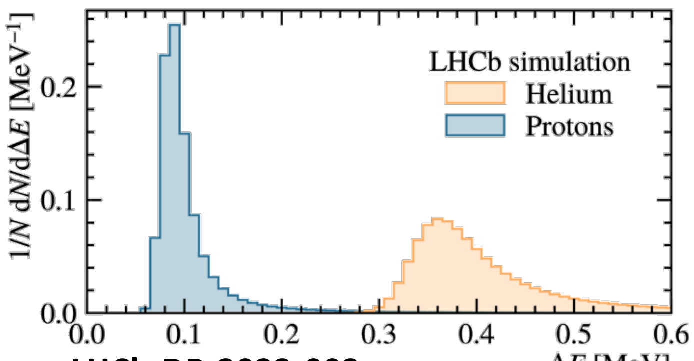

LHCb-DP-2023-002

Bethe-Bloch: Z=2 particles deposits ~4 times the energy of Z=1 particles

→ **He: higher ADC counts and wider cluster size**

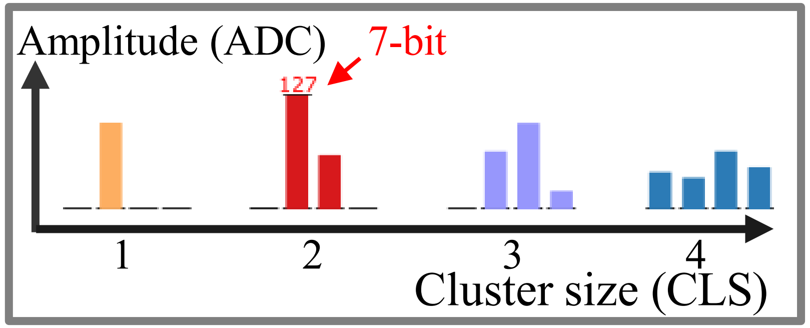

Define Likelihood discriminators based on cluster size and ADC counts:

$$\mathcal{L}^X = \left(\prod_{i=1}^{n} \mathrm{PDD}_i^X\right)^{1/n}, X = \{\mathrm{He}, \mathrm{Bkg}\}$$

$$\Lambda_{\mathrm{LD}} = \log\mathcal{L}^{\mathrm{He}} - \log\mathcal{L}^{\mathrm{Bkg}}$$

One discriminator for each subdetector:

- $\Lambda_{\mathrm{LD}}^{\mathrm{VELO}}$
- $\Lambda_{\mathrm{LD}}^{\mathrm{TT}}$
- $\Lambda_{\mathrm{LD}}^{\mathrm{IT}}$

Probability Density Distributions (PDD)

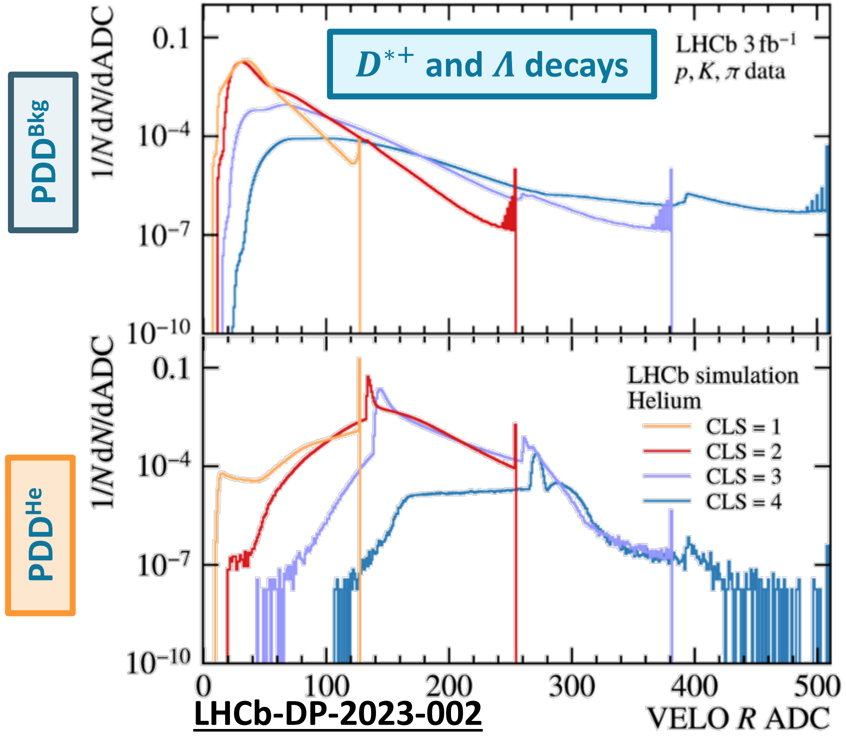

LHCb-DP-2023-002

Prompt (anti-)Helium at LHCb

Selection:

Run2 data: ***pp* collisions at $\sqrt{s} = 13$ TeV**, $\mathcal{L}_{int}$=5.5 fb^{-1}

- All trigger lines
- Prompt tracks (compatible with PV) passing through VELO, TT, and T1->T3
- Good quality tracks ($\chi^2_{track} < 3$, $N_{clusters\ X\ Si\ station}$ >2)
- $p/|Z|$>2.5 GV and $p_T/|Z|$>0.3 GV
- Λ_{LD}^{VELO}>0 and Λ_{LD}^{TT}>-1; Λ_{LD}^{IT}>-1 for IT tracks
- Rejection of photon conversions

First (anti-)Helium candidates observed in *pp* in LHCb data!

LHCb-DP-2023-002

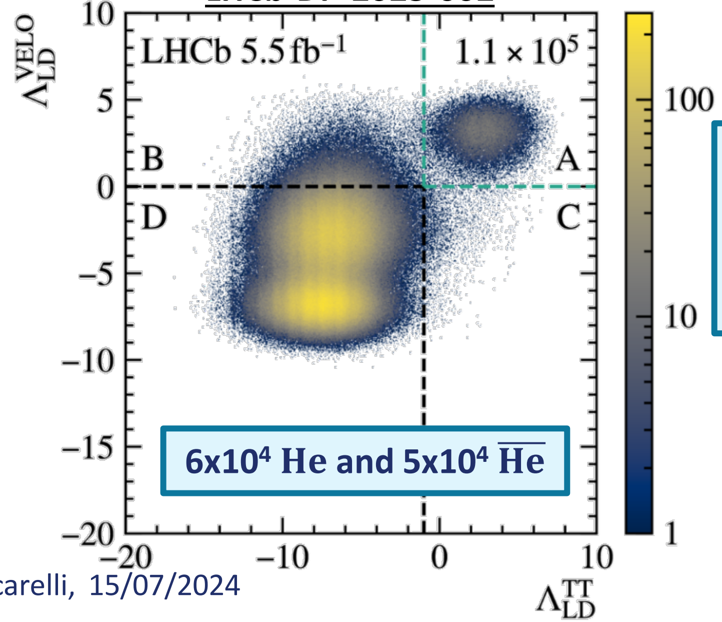

Performance:

- **MisID** probability: $\mathcal{O}(10^{-12})$
- **Signal efficiency**: $\sim$ 50%

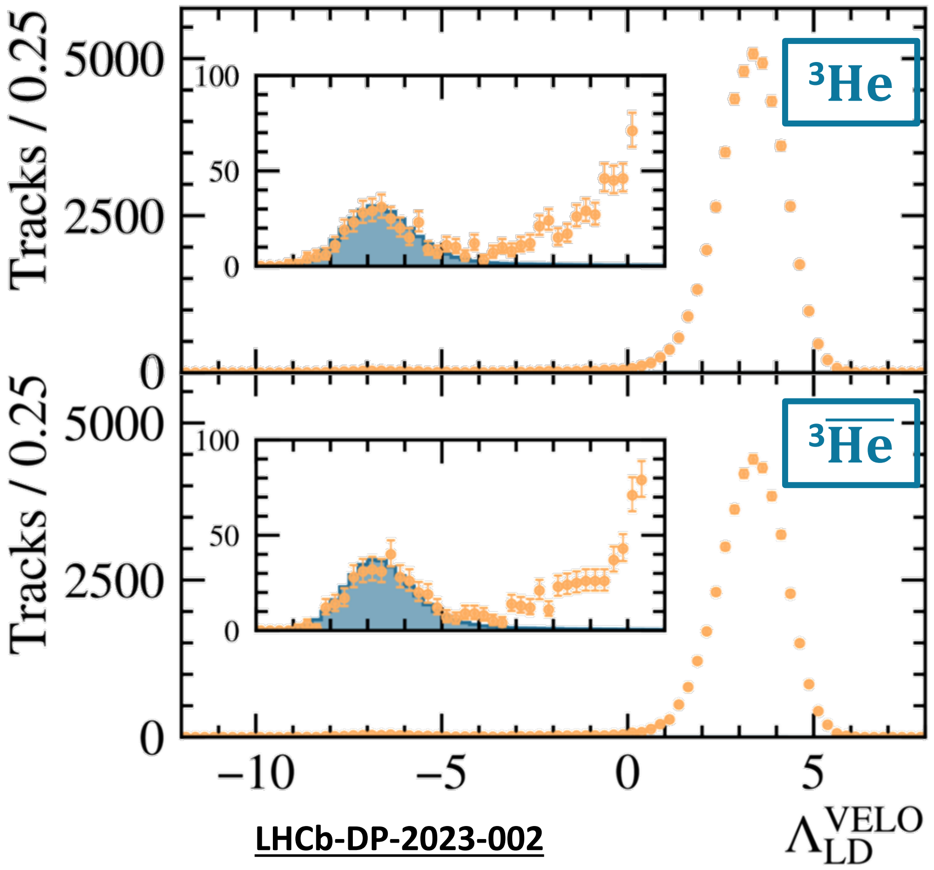

LHCb-DP-2023-002

Application: Hypertriton

- Hypertriton life-time and binding energy gives access to hyperon-nucleon interaction
  → **Constrains on maximum mass of neutron stars**

Search for 2-body decay into He:

$$^{3}_{\Lambda}\mathrm{H} \to {}^{3}\mathrm{He}\,\pi^{-} + cc$$

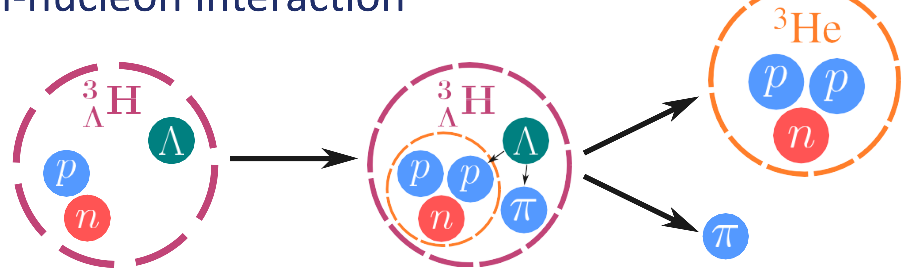

Results:

(Run2 *pp* collisions at $\sqrt{s} = 13$ TeV)

- **Yields**:
  - 61 ± 8 Hypertriton
  - 46 ± 7 anti-Hypertriton
- Statistical **mass precision**: 0.16 MeV

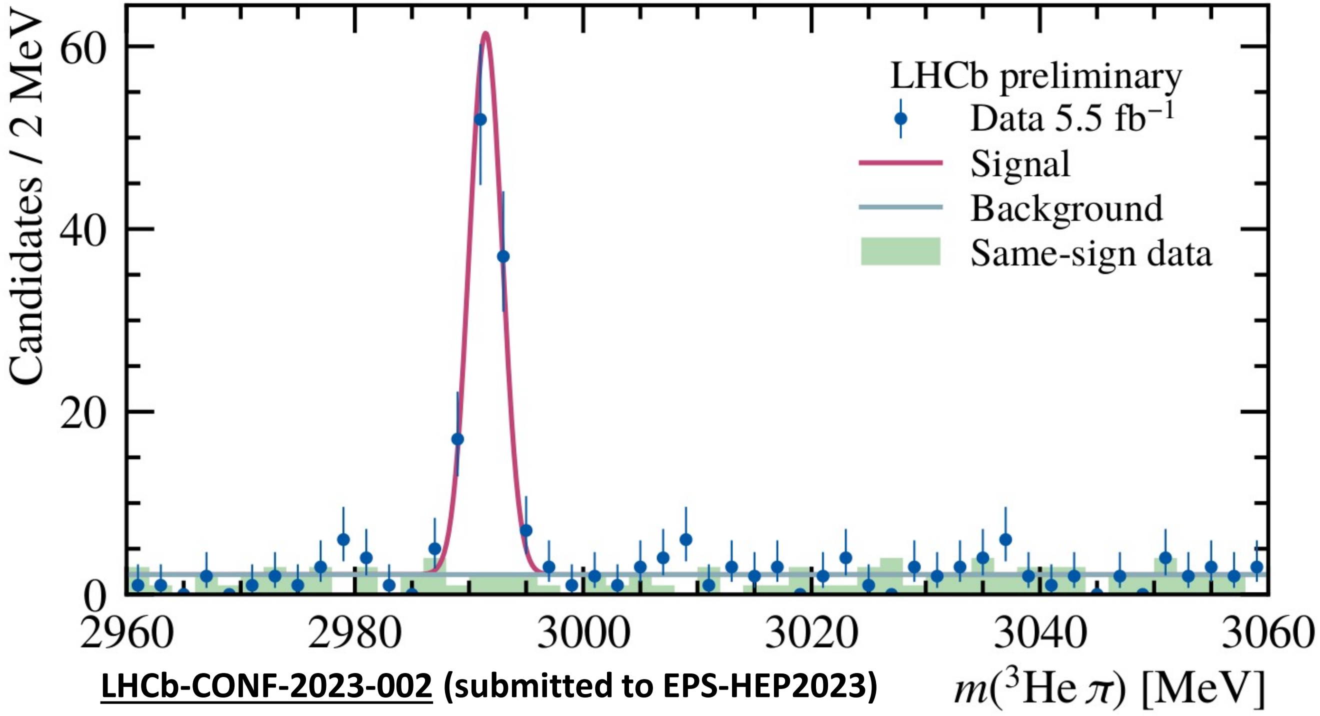

LHCb-CONF-2023-002 (submitted to EPS-HEP2023)

Under investigation:

- Systematic corrections on mass scale:
  - Charge-sign dependent energy-loss
  - Tracking corrections for Z=2
- Efficiency and acceptance corrections

Time-of-flight measurement at LHCb

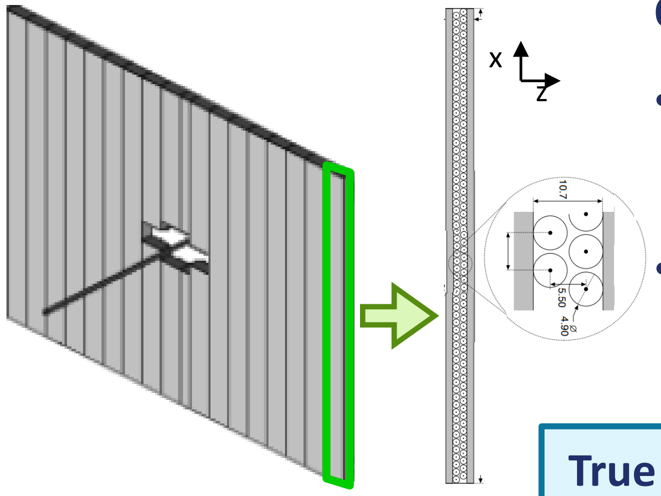

OT (Outer Tracker): largest area, straw-tube drift chambers

- Hit position from ionization cluster t_{drift}– r relation

$$t_{drift} = t_{TDC} - t_{TOF} - t_{prop}$$

- t_{TOF} calculated in the β=1 hypothesis. For β<1:

$$t_{TOF,reco} < t_{TOF,real} \implies t_{drift,reco} > t_{drift,real} \implies \text{r-error}$$

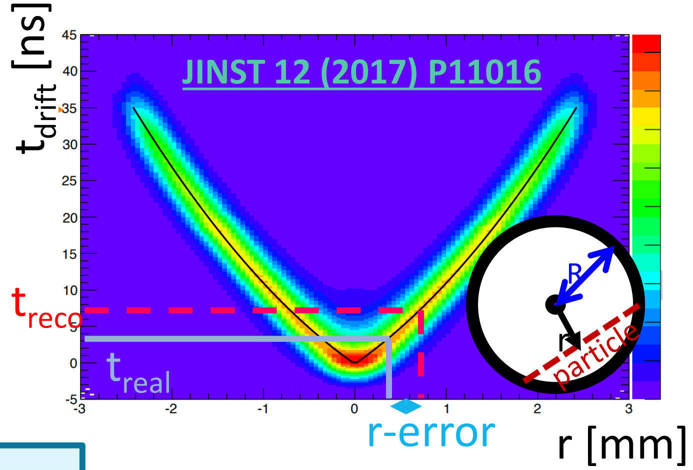

True β minimises the χ^2_{fit} → Particle ID through time measurement

Standard LHCb reconstruction (β=1) inefficient for light nuclei
→ Modified pattern recognition algorithm

Correct hits position to recover reconstruction efficiency

- Loop on $\beta \in \left[1/\sqrt{1 + M^2_{max}/p^2}\,, 1\right]$
- For each β : hits position for β value and perform fit
- Select candidate with best χ^2_{fit}

MC sample:

QGSJET for *p*He + **coalescence afterburner** (1 coal x event)

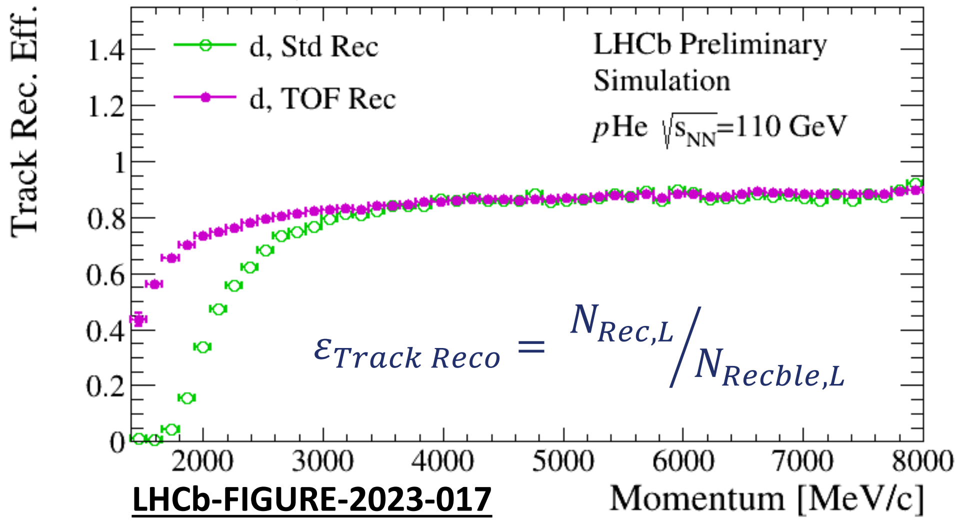

LHCb-FIGURE-2023-017

(Anti-)deuteron identification

Reconstructed tracks refitted to determine β → Iterative procedure rerunning Kalman fit with different β hypotheses

1. At least 15 OT hits required on each track
2. Change β following χ^2_{fit} decrease (gradient descent) without outliers removal → $\chi^2_{\text{fit}} = \chi^2_{\text{track}} + [(\text{t}_{\text{M1}} - \langle\text{M1}\rangle)/\sigma_{\text{M1}}]^2$
3. Fit around minimum to estimate β_{fit} and its uncertainty
4. If fit at minimum has outliers, removed and reiterate procedure

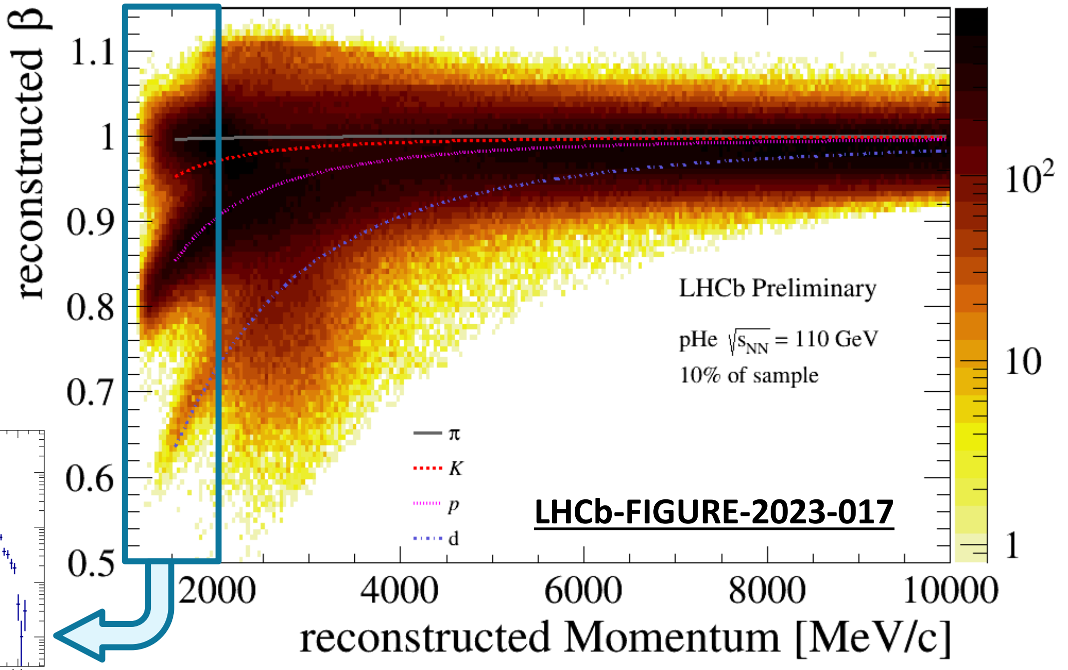

- **~10% of SMOG *p*He** ($\sqrt{s_{NN}}$ = 110 GeV) dataset
- **Background suppression**: σ(β) < 0.02 , χ^2_{OThits}/ndf <2

First deuteron candidates observed in *p*He data!

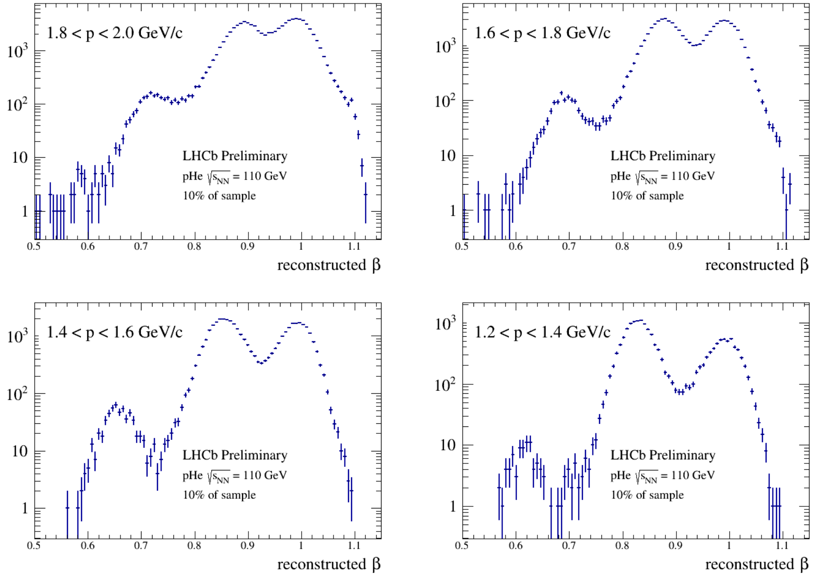

LHCb-FIGURE-2023-017

Under investigation:

- Some DATA/MC discrepancies in OT response
- Efficiencies and systematics studies
- Improve background suppression to expand momentum range where clean identification achievable

Analysis strategy

arXiv:2405.11324, submitted to JHEP

Λ^0 transverse polarization searches exploits the self-analyzing decays

$$\Lambda^0 \longrightarrow p\pi^-$$
$$\bar{\Lambda}^0 \longrightarrow \bar{p}\pi^+$$

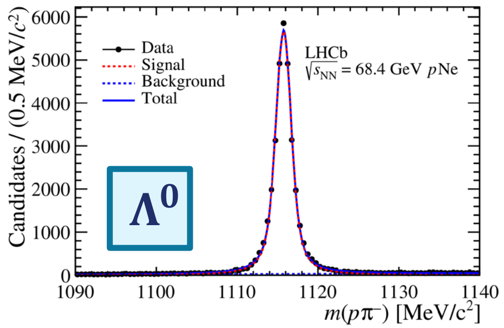

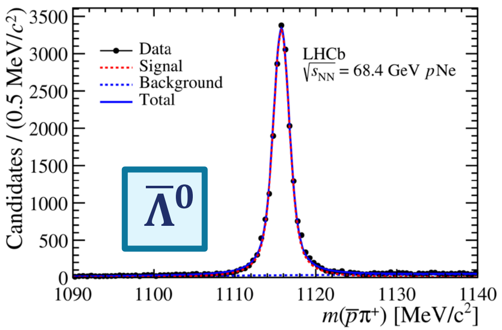

Strong parity violation: p preferentially emitted along the Λ^0 spin direction in its rest frame.

→ Protons angular distribution depends on the Λ^0 polarization P^{Λ^0}:

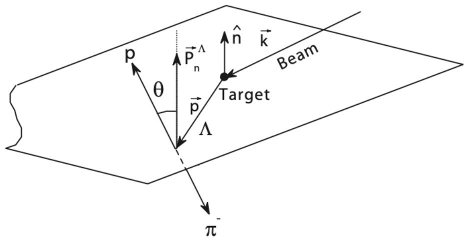

$$\frac{dN}{d\Omega} = \frac{dN_0}{d\Omega}(1 + \alpha P^{\Lambda^0} \cos\theta)$$

$\frac{dN_0}{d\Omega}$: decay distribution for unpolarized Λ^0
α : parity-violating decay asymmetry for Λ^0, fixed to world average
θ : angle between $\bar{p}_p$ and $\hat{n}$ normal to production plane

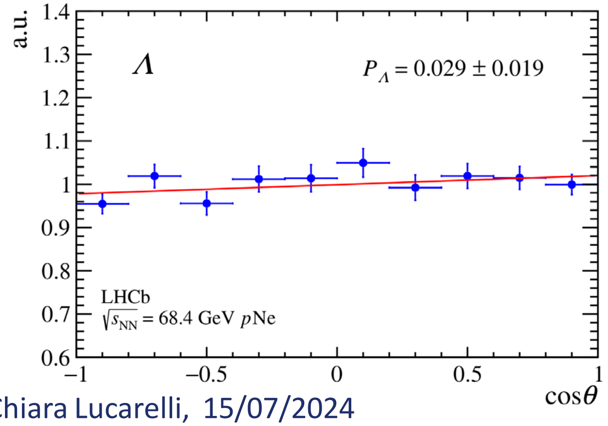

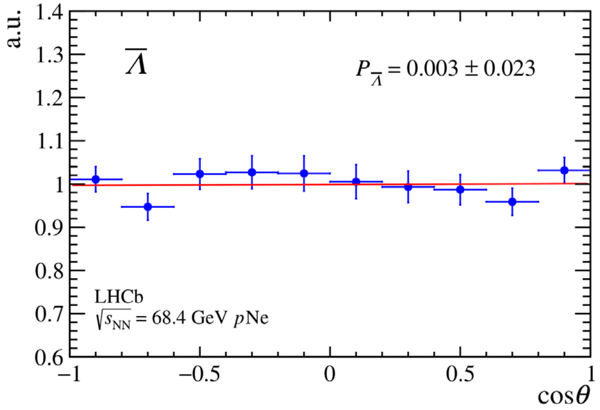

P^{Λ^0}* from linear fit of *p* angular distribution in bin of cos*θ

Polarization studied as a function of the Λ^0 p_T, η, *y* and x_F considering dependence observed in previous studies.

Results

arXiv:2405.11324, submitted to JHEP

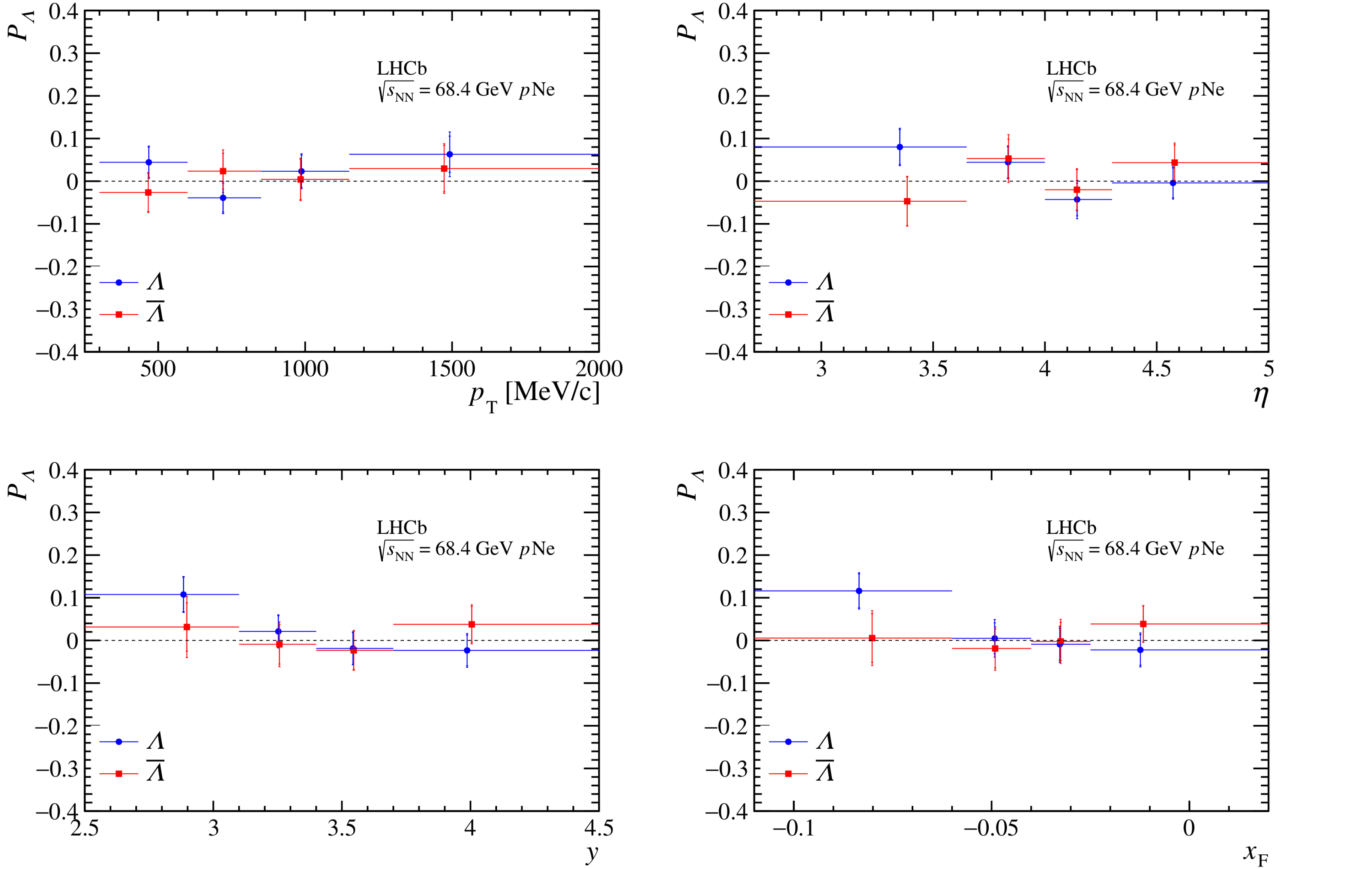

GFS and injection

Gas injected into cell or VELO tank through the Gas Feed System:

- Four gas reservoirs (3 noble gases + 1 non getterable line), used to fill the calibrated volumes V1 and V2, controlled by dosing valve DV601
- Table with calibrated volumes used during injection, pumping group to clean line and dosing valve DV602 to control injected flux.
- Gas feed line to feed either the VELO tank (PV503) or the cell (PV611)
- Turbo pump TP301 connected to VELO tank through GV302 (open during SMOG2 operations) to provide pumping when ion pumps off.

- Multiple gauges to measure pressure along the line and in the VELO tank:
  1. PZ602: pressure at calibration volumes, around 10 mbar when full.
  2. PZ601 and PI601: pressure at the beginning and end of GF line, O(0.01) mbar for SMOG2, O(0.001) mbar a-la-SMOG (PI601 under sensibility).
  3. PE301: pressure at the turbo pump TP301 (SMOG injection point), O(1e-8) mbar for SMOG2, O(1e-6) mbar a-la-SMOG.
  4. PE411 and PE412: pressure in the VELO tank in Ne equivalent, O(1e-8) mbar.